scientific reports

OPEN

A green hydrophobic deep eutectic solvent for extraction of phenol from aqueous phase

Javad Saien✉, Mansoureh Bahiraei & Farnaz Jafari

Deep eutectic solvents (DESs), have been recognized as effective materials for the extraction of different compounds. In this study, the performance of a novel hydrophobic DES was evaluated for the extraction of phenol from aqueous solutions. Octanoic and dodecanoic fatty acid precursors with a definite molar ratio of 3:1, respectively, were used for the DES having a low melting point of 8.3 °C. The purity and stability of the product were confirmed via characterizing by FTIR, ^{1}H and ^{13}C NMR methods. The liquid–liquid equilibrium of the water + phenol + DES ternary system at different temperatures of 293.2, 298.2 and 308.2 K was accordingly studied through cloud point titration method and refractive index measurement. Interestingly, the important parameters of the solute distribution coefficient and the separation factor were, respectively, within the high levels of (6.8321–9.7787) and (895.76–2770.17), indicating the amazing capability of the DES. Reasonably, both of these parameters decreased with temperature. The NRTL and UNIQUAC thermodynamic models were employed to reproduce the obtained tie-lines and to determine the interaction parameters at each temperature. The low level root mean square deviations for the mentioned models were, respectively, within (0.0014–0.0027) and (0.0045–0.0063); confirming satisfactorily agreement with the experimental data.

The extensive generation/utilization of phenol in various industries like refineries, petrochemical industries, coal gasification, pulp and paper, paint, pharmaceutical, plastics and resin has leaded to generating huge phenolic wastewaters. Non desired effects of phenol on the environment and human is mainly attributed to its toxicity and hazardous nature. Thus it seems quite beneficial to process wastewaters for separating phenol/phenolic compounds[1].

Two main strategies for removing phenol from wastewater, reported by the investigators, are (i) degradation via wet oxidation, electrochemical and photocatalytic oxidation and (ii) separation via membrane, extraction and adsorption. Both of these strategies have the benefits and drawbacks. Indeed, recovery and reusability of phenol is not feasible in degradation strategy[2].

Among various separation techniques such as liquid–liquid extraction, azeotropic distillation and extractive distillation; the latter, due to forming a binary azeotrope between water and phenol, is challenging and thus, liquid–liquid extraction is usually preferred[3]. In this regard, selecting an optimal solvent according to the main criteria of miscibility gap, separation capability, selectivity, environmental friendly and availability is important. In this regard, the undesired properties of most of the volatile conventional solvents such as flammability, toxicity, and regeneration problems have persuaded the researches to design and create novel solvents to overcome these problems[4,5].

Accordingly, ionic liquids (ILs) and deep eutectic solvents (DESs) as new generations of green solvents have been introduced with desirable properties, e.g. low vapor pressure, non-flammability, biocompatibility and wide liquid phase range[6,7]. Worth mentioning that DESs, in comparison with ionic liquids, have the advantages of easier and cheaper preparation, more biodegradability and less toxicity[8].

Generally, DESs consist of two or three substances, hydrogen bound donor (HBD) and hydrogen bound acceptor (HBA), bringing about a melting point of less than each substance[9]. In this regard, a typical DES, introduced by Abbot[10] (2001), was made of choline chloride (HBA) and urea (HBD) with molar ratio of 1:2. Meanwhile, The limitation of utilizing hydrophilic DESs in polar systems encouraged Van Osch et al.[11] (2015) to propose the first series of hydrophobic DESs for extraction process. Table 1 summarizes the recent investigations on using hydrophobic DESs in the extraction process. Since the involved components significantly influence the DES physico-chemical characteristics, the long hydrocarbon chains e.g. C_8 and longer fatty acids with the unique

Department of Chemistry and Petroleum Science, Bu-Ali Sina University, Hamedan, Iran. ✉email: saien@basu.ac.ir

HBA	HBD	Molar ratio	Reference
Tetraoctylammonium bromide	Decanoic acid	2:1	[11]
Methyltrioctylammonium bromide	Decanoic acid	2:1	
Methyltrioctylammonium chloride	Decanoic acid	2:1	
Tetraoctylammonium chloride	Decanoic acid	2:1	
Tetraheptylammonium chloride	Decanoic acid	2:1	
Tetrabutylammonium chloride	Decanoic acid	2:1	
Menthol	Dodecanoic acid	2:1	[16,17]
Menthol	Palmitic acid	12:1	[18]
n-tetraoctylammonium bromide	Decanoic acid	2:1	[19]
Thymol	Decanoic acid	1:1	
Menthol	Decanoic acid	1:1	
Dodecanoic acid	Menthol	several	[20]
n-nonanoic acid	Menthol	2:1	
Decanoic acid	Menthol	2:1	
Undecanoic acid	Menthol	2:1	
Dodecanoic acid	Decanoic acid	1:2	[14]
Dodecanoic acid	Octanoic acid	1:3	[21]
Dodecanoic acid	Nonanoic acid	1:3	
Thymol	Octanoic acid	1:2	[22]
Menthol	Octanoic acid	1:2	
Thymol	Hexanoic acid	1:1	[23]
Thymol	Heptanoic acid	1:1	
Thymol	Octanoic acid	1:1	
Thymol	Nonanoic acid	1:1	

Table 1. The list of studies on the using of hydrophobic DESs in liquid–liquid extraction.

properties of non-toxicity and biodegradability[12,13] are preferred as precursors for preparing DESs[14]. It is while, those made of short hydrocarbon chain fatty acids are usually unstable in water[15].

The desired properties of DESs such as low viscosity and density, flammability and vapor pressure, water immiscibility and stability are remarkable. On the other hand, in order to optimize and simulate the liquid–liquid extraction process, ternary diagrams of the liquid–liquid equilibrium (LLE) must be presented. Here, a novel DES, prepared from octanoic acid (C_8) and dodecanoic acid (C_{12}) precursors was prepared and characterized via FTIR spectroscopy as well as ^1H and ^{13}C NMR analyses. Afterward, the phenol extractability by the proposed DES was scrutinized at different temperatures. Othmer-Tobias, Hand, and Bachman well-known equations were employed to confirm the tie-lines consistency. Using the Aspen Plus simulator, the tie-line data were regressed using the well-known NRTL and UNIQUAC thermodynamic models. For this aim, regarding the composition complexity of the DES; a pioneering novel approach, based on group contribution, was employed for correlating the tie-lines and obtaining the binary interaction parameters.

Experimental
Materials
The fatty acid precursors of dodecanoic acid and octanoic acid were purchased from Sigma – Aldrich. Phenol was supplied from Merck and used without additional purification. A water deionizer apparatus (Hastaran, Iran) produced fresh deionized water with conductivity of less than 0.08 μS/cm, utilized for preparing solutions. The chemical names along with other related information are listed in Table 2.

Chemical	CAS No	Supplier	Purity
Water	7732 – 18 – 5	Hastaran	Ultrapure
Phenol	108 – 95 – 2	Merck	> 99%
Octanoic acid	124 – 07 – 2	Sigma – Aldrich	≥ 98%
Dodecanoic acid	143 – 07 – 7	Sigma – Aldrich	98%

Table 2. Specification of the utilized chemicals.

## Preparation of DES and solid – liquid phase diagram

Different molar ratios of C_8 and C_{12} carboxylic acids were gradually heated in a jacketed glass vessel up to 70 °C while magnetic stirring until reaching a homogeneous and clear solution of single phase[21,24]. The samples were prepared by mass using an Ohaus balance (Adventurer, Pro AV264, Switzerland, uncertainty 0.0001 g). Consequently, temperature was gradually reduced until the first evidences of solid phase was observed at a certain temperature. The corresponding solid – liquid phase diagram of the DES, illustrated in Fig. 1, shows obtaining a specific DES from octanoic and dodecanoic fatty acids with certain molar ratio of 3:1 (0.25 mol fraction of dodecanoic acid). It can be seen that the melting point of the DES (8.3 °C) is much lower than octanoic acid (16.5 °C) and dodecanoic acid (43.2 °C) bringing about a stable liquid state product for operations under conventional temperatures.

The eutectic product was characterized by FTIR (Perkin Elmer FTIR spectrometer, USA) , ^{1}H and ^{13}C NMR analysis[16,21] (Varian – Inova 500 MHz NMR, USA) using dimethyl sulfoxide (DMSO-d6) as solvent. The density and refractive index of the prepared DES and water were measured, respectively, with an oscillating densimeter (Anton Paar DMA4500, Austria) with a relative uncertainty of 0.001, and a refractometer (Abbe AR4 Kruss, Germany) with uncertainty of 0.0007. The obtained values and those reported in literatures are compared in Table 3, indicating a close agreement. Ensuring the stability of the DES in aqueous media, 50% volume ratio in water were stirred for 8 h and was left settling overnight. Therefore, both phases were thoroughly in contact and were separated.

Solubility and LLE measurements

The basis of experiments in LLE experiments was the cloud-point titration and refractometry methods. Although various analytical methods have been developed to measure the concentration of components e.g., gas chromatography (GC) and high performance liquid chromatography (HPLC)[29,30], the most applicable approach to determine the solubility of liquids is cloud point titration, also known as "turbid point titration". The method has advantages of easily operation, high accuracy and cost effective. An extensive discussion about the conventional methods in LLE analysis has been recently reported by Arce et al.[31]. This approach has been used extensively in recent publications[32,33]. Noteworthy, the visual detection of turbidity and end-point of titration, and the requirement of a calibration curve are the limitation of this analytical method.

For analysis, a set up consisted of a miniature jacketed vial with approximated volume of 5 cm³, refractometer, thermostat (Julabo, Germany, uncertainty of 0.01 K) and magnetic stirrer were used. A water stream was circulated by a thermostat driving pump through the jacket and refractometer for maintaining temperature at a
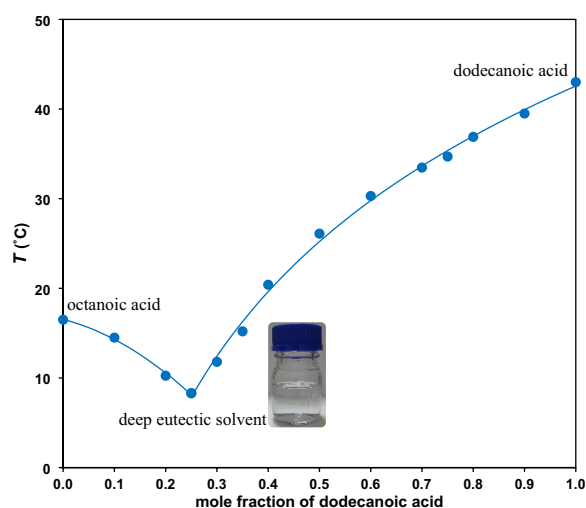
Figure 1. Solid – liquid phase diagram for octanoic and dodecanoic fatty acid precursors.

Component	n_d		ρ (g/cm³)	
	Exp	Lit	Exp	Lit
Water	1.33250	1.33250[25,26]	0.99705	0.99704[27]
				0.99693[28]
DES	1.43050	1.42967[21]	0.90064	0.90100[14]
				0.90110[21]

Table 3. Refractive index and density for water and the DES at temperature of 298.2 K and under atmospheric pressure of 81.5 kPaᵃ. ᵃAverage uncertainties are $u(T) = 0.1$ K, $u(n_d) = 0.0007$, and $u_r(\rho) = 0.001$.

certain value. Temperature of the thermostat was calibrated via a reference thermometer (Amadigit, Germany, uncertainty 0.01 K).

Firstly, to determine the calibration curves (relationships between the concentration of each component and the refractive index), the binary mixtures of (water + phenol) or (DES + phenol) with specific amounts were prepared by means of the Ohaus balance. The next step was titrating of the binary mixtures, being stirred at a constant temperature, by precise addition of the remained component (DES or water) via a micro-siring until threshold of a stable cloudy solution. Then, the content was weighed to determine the amount of the third component and refractive index for the cloudy solution was measured immediately. In this way, the calibration curves were attained under atmospheric pressure of 81.5 kPa and different temperatures. In the Supporting materials (Table S1), the calibration curves and related data are presented. It can be seen in Figs. S1 and S2 that the refractive index of cloudy solutions increases with the phenol mass transfer which is attributed to its higher refractive index value.

The equilibrium cells containing different samples with specific and accurate amounts of involved components (water, phenol and DES) were tightly closed. These were agitated in a shaking water bath (N − BIOTEK − 304, South Korea, uncertainty of 0.1 K) at constant temperature and 175 rpm under ambient pressure for 4 h, then the phases were completely separated by resting more than 12 h time.

Collecting the organic phase (top) and aqueous phase (bottom) samples with a syringe, the related refractive indices were determined. It is worth noting that ensuring the accurate experimental data, the analysis of each sample was repeated three times. Using aqueous and organic phase calibration curves and the corresponding refractive indices, the mass fraction of each component with the uncertainty of 0.0002 except $u(w_{31})$ and $u(w_{11})$ as 0.0003 was determined. Table 4 presents the tie-line data at different temperatures.

The DES capability for selective separation of phenol was evaluated from separation factor (S) criterion:

$$S = \frac{D_2}{D_1} \tag{1}$$

where D_1 is the water distribution coefficient and D_2 the phenol distribution coefficients obtained from:

Aqueous phase			Organic phase					
w_{11}	w_{21}	w_{31}	w_{13}	w_{23}	w_{33}	D_1	D_2	S
$T = 293.2$ K								
0.9932	0.0042	0.0026	0.0035	0.0406	0.9559	0.0035	9.7787	2770.17
0.9885	0.0090	0.0025	0.0038	0.0765	0.9197	0.0039	8.4983	2205.24
0.9858	0.0118	0.0024	0.0040	0.0961	0.8999	0.0041	8.1368	1989.05
0.9814	0.0164	0.0022	0.0043	0.1262	0.8695	0.0044	7.6931	1745.39
0.9785	0.0194	0.0021	0.0046	0.1462	0.8492	0.0047	7.5361	1618.77
0.9755	0.0225	0.0020	0.0048	0.1684	0.8268	0.0049	7.4844	1528.61
0.9726	0.0255	0.0019	0.0050	0.1897	0.8053	0.0052	7.4392	1437.83
0.9701	0.0281	0.0018	0.0052	0.2084	0.7864	0.0053	7.4164	1392.21
$T = 298.2$ K								
0.9928	0.0043	0.0029	0.0042	0.0395	0.9563	0.0042	9.2045	2198.14
0.9880	0.0093	0.0027	0.0045	0.0741	0.9214	0.0046	8.0045	1744.67
0.9850	0.0124	0.0026	0.0048	0.0943	0.9009	0.0049	7.6091	1547.12
0.9807	0.0168	0.0024	0.0052	0.1248	0.8700	0.0053	7.4154	1407.73
0.9770	0.0208	0.0023	0.0054	0.1527	0.8419	0.0056	7.3573	1321.84
0.9742	0.0236	0.0022	0.0057	0.1729	0.8214	0.0059	7.3181	1246.45
0.9714	0.0265	0.0021	0.0060	0.1931	0.8009	0.0061	7.2863	1188.31
0.9681	0.0299	0.0020	0.0062	0.2162	0.7776	0.0064	7.2304	1125.02
$T = 308.2$ K								
0.9928	0.0043	0.0029	0.0053	0.0365	0.9583	0.0053	8.8729	1676.23
0.9880	0.0093	0.0027	0.0056	0.0670	0.9274	0.0057	7.8353	1379.55
0.9850	0.0124	0.0026	0.0060	0.0964	0.8977	0.0061	7.2643	1197.67
0.9807	0.0168	0.0024	0.0063	0.1217	0.8699	0.0064	7.0973	1104.71
0.9770	0.0208	0.0023	0.0066	0.1486	0.8480	0.0067	6.9739	1037.36
0.9742	0.0236	0.0022	0.0068	0.1674	0.8241	0.0070	6.9513	988.25
0.9714	0.0265	0.0021	0.0071	0.1931	0.7997	0.0074	6.9065	938.47
0.9681	0.0299	0.0020	0.0074	0.2157	0.7797	0.0076	6.8321	895.76

Table 4. Experimental tie-line mass fractions (w) for water (1) + phenol (2) + DES (3) along with distribution coefficient of water (D_1), of phenol (D_2) and separation factor of phenol (S) at different temperatures and under atmospheric pressure 81.5 kPa[a]. [a]Standard uncertainties are: $u(p) = 0.3$ kPa, $u(T) = 0.1$ K, $u(n_d) = 0.0007$, and $u(w) = 0.0002$ except $u(w_{33}) = u(w_{11}) = 0.0003$.

$$D_1 = \frac{w_{13}}{w_{11}} \tag{2}$$

$$D_2 = \frac{w_{23}}{w_{21}} \tag{3}$$

The greater than unity values of the separation factor and distribution coefficient confirms the capability of the DES for extraction of phenol. A higher D_2 is desired because of a higher extracted solute. In other words, less solvent is required to achieve a specific extraction. Also, S indicates the separation possibility and the solvent selectivity for the solute extraction[5,34].

Results and discussion
DES characterization
The FTIR spectra of the DES just after preparation and after mixing with water, are presented in Fig. S3. As can be seen, there is no change in DES structure after mixing with water. ^{1}H and ^{13}C NMR spectra are also given in Supporting materials (Figs. S4 and S5), respectively. Considering no additional peak after mixing with water, it can be concluded that there was no chemical reaction or dissociation of fatty acids, i.e. stable in contact with water. Also, the lack of the precursor peaks in the FTIR and ^{1}H NMR of water phase (Fig. S6) confirms again the stability. The summary of the DES analysis data is given in Table 5.

Tie-line results
The tie-line data for the ternary system of water + phenol + DES at different temperatures of 293.2, 298.2 and 308.2 K are listed in Table 4. Corresponding phase diagrams are presented in Fig. 2. In general, mass fractions of the ith component of water = 1, phenol = 2 and DES = 3 are presented as w_{i1} and w_i in the aqueous and organic (DES) phases, respectively. Regarding immiscibility of water and DES, partial miscibility of water and phenol as well as DES and phenol, the investigated system is assigned as a type − 2 LLE system[35].

As illustrated in Fig. 2, the higher solubility of the solute in the DES phase is consistent with the slope of the obtained tie-lines and can be attributed to the potential hydrogen bonding between phenol and the DES[36,37]. With respect to temperature effect, a gradual diminishing of the binary area is observed with increasing temperature. This can be attributed to the little miscibility tend of water and DES and to some extent, decreasing the phenol hydrogen bound with the DES[38]. It is necessary to mention that the effect of temperature is more evident at higher concentrations of the solute. The same results were previously reported for several chemical systems, for instance, water + phenol + imidazolium ionic liquid[36], water + phenol + cumene[27] and water + acetone + HMIMPF$_6$ IL[39].

### Distribution coefficients and selectivity criteria
The distribution coefficients are presented in Figs. 3 and 4, and the separation factor in Fig. 5. The phenol distribution coefficient lies within the range (6.8321–9.7787) and the separation factor within (895.76–2770.17). These confirm the amazing capability of the DES for phenol extraction. The comparison of separation factor ranges of DES with several other solvents, examined for separation phenol from water, at a typical temperature of 298.2 K, is provided in Table 6. There is significantly higher separation factor for the DES than ILs and some

Component	Condition	Spectrums	Details
DES	After preparation	FTIR	The peaks at 2856 cm^{-1} and 2926 cm^{-1} represents the stretching of —CH$_2$ and —CH$_3$ vibrations The peak at 1466 cm^{-1} represents the deformation vibration of —CH2 or —CH3 groups The peak at of 1712 cm^{-1} represents the stretching vibration of C = O The peak at of 1285 cm^{-1} represents stretching vibration of C—O The peak at of 938 cm^{-1} represents the stretching vibration of —OH
		^{1}H NMR	δ (ppm) = 0.83 (6H, 2CH$_3$), 1.22 (24H, 12CH$_2$), 1.47 (4H, 2CH$_2$), 2.14 (4H, 2CH$_2$), 2.49 (DMSO-d$_6$), 11.87 (2H, 2OH)
		^{13}C NMR	δ (ppm) = 14.16, 22.52, 24.95, 29.04, 31.66, 34.06, 39.57, 174.72
	After mixing with water	FTIR	The peaks at 2856 cm^{-1} and 2927 cm^{-1} represents the stretching of —CH$_2$ and —CH$_3$ vibrations The peak at 1466 cm^{-1} represents the deformation vibration of —CH2 or —CH3 groups The peak at of 1712 cm^{-1} represents the stretching vibration of C = O The peak at of 1285 cm^{-1} represents stretching vibration of C—O The peak at of 937 cm^{-1} represents the stretching vibration of —OH
		^{1}H NMR	δ (ppm) = 0.83 (6H, 2CH$_3$), 1.22 (24H, 12CH$_2$), 1.47 (4H, 2CH$_2$), 2.14 (4H, 2CH$_2$), 2.49 (DMSO-d$_6$), 11.87 (2H, 2OH)
		^{13}C NMR	δ (ppm) = 14.15, 22.52, 24.95, 28.94, 31.66, 34.06, 39.89, 174.72
Water	After mixing with DES	FTIR	The peaks at 3435 cm^{-1} represents the stretching vibration of O—H The peaks at 1637 cm^{-1} represents the bending vibration of O—H
		^{1}H NMR	δ (ppm) = 2.49 (DMSO-d$_6$), 3.53 (2H, 2H$_2$O)

Table 5. FTIR, ^{1}H NMR and ^{13}C NMR spectrums specification for DES and water phases.
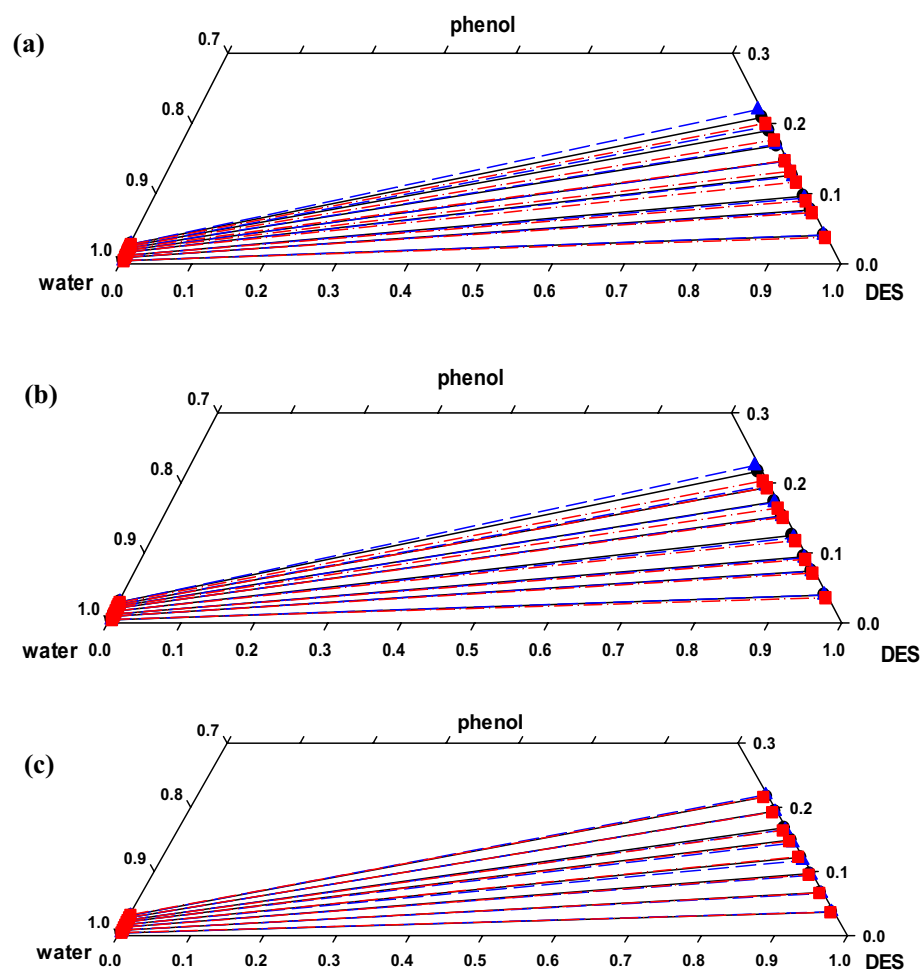
Figure 2. Ternary diagrams of (water + phenol + DES) system at $T = 293.2$ (**a**), 298.2 (**b**) and 308.2 (**c**) K; ● and solid lines experimental, ▲ and dashed lines NRTL predicted tie-lines, ■ and dash-dotted lines UNIQUAC predicted tie-lines.
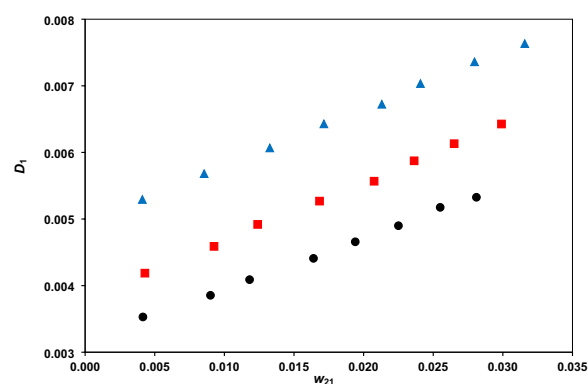

Figure 3. The water distribution coefficients vs. phenol mass fraction at temperatures of 293.2 K (●), 298.2 K (■) and 308.2 K (▲).

other conventional solvents. Indeed, the higher separation factor of methyl tert-butyl ketone should be regarded with the environmental issues which limits the applications.

The separation factor decreases with increasing phenol mass fraction in aqueous phase (Fig. 5). The reason is relevant to the fact that the water content in the organic DES phase increases with solute concentration. On the other hand, increasing temperature leads to a lower separation factors because of weakening the hydrogen
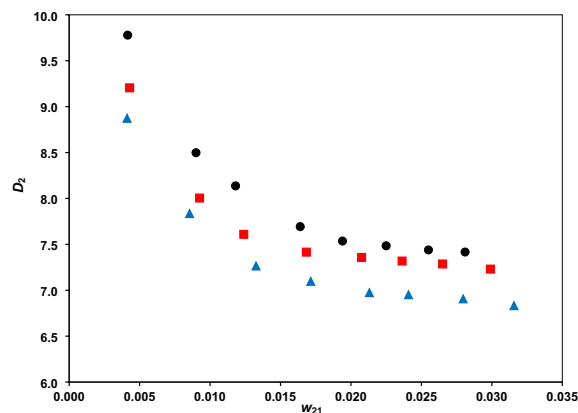
Figure 4. The phenol distribution coefficients of vs. its mass fraction at temperatures of 293.2 K (●), 298.2 K (■) and 308.2 K (▲).
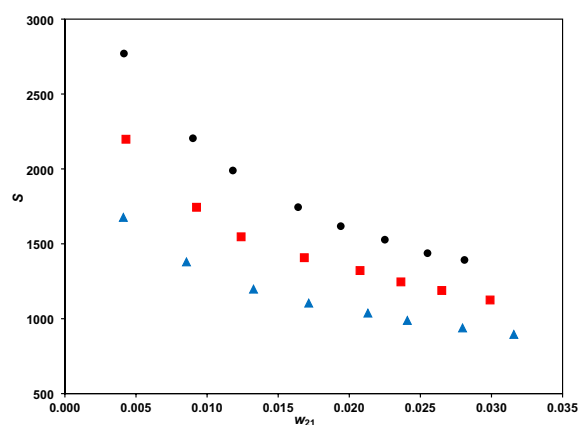
Figure 5. The DES separation factor vs. phenol mass fraction at different temperatures of 293.2 K (●), 298.2 K (■) and 308.2 K (▲).

System	Solvent	Separation factor (Ref.)
Water + phenol + cumene	Cumene	93.41–240.58[27]
Water + phenol + imidazolium IL	[Hmim][NTf2]	134.68–948.75[36]
Methyl tert – butyl Ketone + phenol + water	Methyl tert – butyl ketone	1334–3953[40]
Water + phenol + dibutyl ether	Dibutyl ether	50.53–1182.39[41]
Water + phenol + 1-octanol	1-octanol	99.5–495.5[42]
Water + phenol + cyclohexanone	Cyclohexanone	126.3–168.0[42]
Water + phenol + 2-ethyl-1-hexanol	2-ethyl-1-hexanol	131.9–398.1[42]
Mesityl oxide + phenol + water	Mesityl oxide	1007–2599[43]
Choline IL + phenol + water	[choline][NTF2]	27.8–41.3y[44]
Water + phenol + DES	DES	1125.02–2198.14 (present work)

Table 6. Separation factor for several solvents in phenol extraction from aqueous phase at 298.2 K.

bond between phenol and the DES[38]. Figure 6 presents the phenol equilibrium distribution between the organic (DES) and aqueous (water) phases at different temperatures, showing rather linear variations.

Consistency tests
The reliability of the experimental data was evaluated based on the Othmer – Tobias, Hand and Bachman well-known correlations as
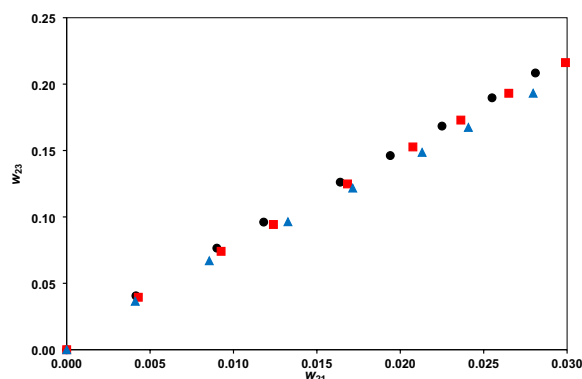
Figure 6. Equilibrium distribution of phenol between the DES and water phases at different temperatures of 293.2 K (●), 298.2 K (■) and 308.2 K (▲).

$$\ln\left(\frac{1-\text{w}_{33}}{\text{w}_{33}}\right) = A_1 + B_1 \ln\left(\frac{1-\text{w}_{11}}{\text{w}_{11}}\right) \tag{4}$$

$$\ln\left(\frac{\text{w}_{21}}{\text{w}_{11}}\right) = A_2 + B_2 \ln\left(\frac{\text{w}_{23}}{\text{w}_{33}}\right) \tag{5}$$

$$w_{33} = A_3 + B_3\left(\frac{w_{33}}{w_{11}}\right) \tag{6}$$

where A_1 and B_1, A_2 and B_2, and A_3 and B_3 are, respectively, intercepts and slopes of the Othmer – Tobias, the Hand and the Bachman correlations[31]. The value of intercepts, slopes and related determination coefficients (R^2) are tabulated in Table 7. The close to unity determination coefficient verifies the tie-line data consistency.

Correlation models

The consistency of the attained ternary data against the NRTL and UNIQUAC thermodynamic models was checked by utilizing Aspen Plus (V. 8.4) simulator through introducing DES as a pseudo component. Hence, the physico-chemical properties of the DES including normal boiling point, molecular weight and density were introduced to the software. For this aim the method proposed by Mirza et al.[45] was employed. Relevantly, simultaneous utilization of the modified Lydersen – Joback – Reid (LJR) method along with the mixing rules has been proposed for critical properties estimation as well as normal boiling points. The accuracy of the method has been tested for 39 different DESs[46]. In this regard, group contribution method and the type and frequency of the groups of atoms were considered. The contributions are summed to obtain the final estimate of the boiling point as

$$T_b = 198.2 + \sum n_i \Delta T_{bMi} \tag{7}$$

where T_b (K), n_i and ΔT_{bMi}(K) are, respectively, the normal boiling point of a DES, the frequency of appearance of the ith group of atoms in the molecule, and group contribution in boiling point for the modified LJR method[45]. Based on Eq. (7) the DES normal boiling point was obtained as 551.0 K.

In the NRTL thermodynamic model, the non-randomness parameter (α_{ij}) was considered to be 0.2 and 0.3[47]. In the UNIQUAC model, the r_i parameter of the number of segments in each molecule and the q_i parameter of the relative surface area per molecule are listed in Table 8[48].

The corresponding interaction parameters of the both models at different temperatures are listed in Table 9. In a previous study, the proper description of the binary interaction parameters are provided[49]. The LLE phase diagram of ternary system based on the obtained data and those of the predicted values by the models are depicted in Fig. 2. Obviously, the models reasonably fit the experimental data.

T (K)	Othmer – Tobias			Hand			Bachman		
	A_1	B_1	R^2	A_2	B_2	R^2	A_3	B_3	R^2
293.2	2.7150	1.1596	0.9995	−2.1192	1.0238	0.9958	−0.1206	1.1181	0.9999
298.2	2.8509	1.2053	0.9997	−2.0861	1.0592	0.9970	−0.1196	1.1162	0.9999
308.2	2.8305	1.2218	0.9992	−2.0416	1.0377	0.9968	−0.1294	1.1259	0.9999

Table 7. The parameters for Othmer – tobias, Hand and Bachman correlations and the corresponding regression coefficients for (water + phenol + DES) system at different temperatures.

8

Component	r	q
Water	0.0092	1.4000
Phenol	3.5517	2.6800
DES	27.6928	23.4080

Table 8. UNIQUAC structral parameters.

T (K)	i − j	NRTL				UNIQUAC		
		b_{ij}(K)	b_{ji}(K)	α_{ij}	RMSD	a_{ij}(K)	a_{ji}(K)	RMSD
293.2	1 − 2	1022.69	465.63	0.2	0.0027	199.22	−2655.13	0.0063
	1 − 3	2299.76	735.93	0.3		175.98	−1146.29	
	2 − 3	−780.80	1129.03	0.3		306.63	−411.06	
298.2	1 − 2	1008.16	416.85	0.3	0.0020	480.09	−1098.45	0.0058
	1 − 3	2339.33	677.67	0.2		178.22	−1106.37	
	2 − 3		−757.61	1057.36	0.2		227.34	−214.64
308.2	1 − 2	1027.34	393.92	0.3	0.0014	527.04	−712.97	0.0045
	1 − 3	2322.88	642.03	0.3		181.39	−1101.86	
	2 − 3	−821.307	1077.02	0.3		180.86	−170.61	

Table 9. Interaction parameters obtained from NRTL and UNIQUAC models for water (1) + phenol (2) + DES (3) system at different temperatures.

The comprehensive root mean square deviation (RMSD) values were determined from the following equation for each of the investigated models and listed Table 9.

$$RMSD = \sqrt{\frac{\sum_i \sum_m \sum_n (w_{imn}^{exp} - w_{imn}^{cal})^2}{6N}} \tag{8}$$

where w_{imn}^{exp} and w_{imn}^{cal} represent the experimental and the model predicted mass fractions, respectively. Here, the subscripts of $i = 1, 2, 3$ are for the components and $m = $ I, II are for the aqueous and organic phases. Further, the $n = 1, 2, …, N$ subscript stand for the number of tie-lines. As shown in Table 9, the RMSD values are very low for the NRTL model within (0.0014–0.0027) and for the UNIQUAC within (0.0045–0.0063). Therefore, the more appropriate model for predicting the tie-line data is the NRTL model

Conclusions

Utilizing a novel hydrophobic DES, consisted of octanoic and dodecanoic acid precursors, the extraction of phenol from aqueous phase was feasible at different temperatures. The liquid state DES was stable for satisfactory extraction operations. Liquid–liquid equilibrium experiments were performed based on the cloud point titration method and refractive index measurements. The results revealed that low amounts of the DES was required for a specific task and that the tie-lines were with positive slopes since phenol tends to be more in the organic phase. Relevantly, the distribution coefficient and separation factor confirmed the high capacity and selectivity of the DES compared to the conventional organic solvents. Higher separation factors were corresponding to the lower temperature which can be attributed to forming hydrogen bond between phenol and the DES. Meanwhile, the consistency of tie line data was appropriately assessed by the Othmer – Tobias and Bachman equations. Finally, the data were correlated by employing a pioneering approach in group contribution calculations relevant to the thermodynamic models of NRTL and UNIQUAC. The appropriate low RMSD values, particularly for the NRTL model, confirmed good agreement with the experimental data.

To extend investigations, capability of the DES in mass transfer of phenol extraction could be scrutinized. For this aim, the viscosity of the solvent and the molecular diffusivity of phenol in the solvent have to be considered.

Data availability

Correspondence and requests for data and materials should be addressed to J.S.

References

1. Jiao, T. *et al.* Separation of phenol and pyridine from coal tar via liquid–liquid extraction using deep eutectic solvents. *Chem. Eng. Res. Des.* **145**, 112–121 (2019).
2. Beradinelli, S., Resini, C. & Arrighi, L. Technologies for the removal of phenol from fluid streams. *J. Haz. Mater.* **160**, 265–288 (2008).

3. Xie, Y. *et al.* Exploring bubble oscillation and mass transfer enhancement in acoustic-assisted liquid-liquid extraction with a microfluidic device. *Sci. Rep.* **5**, 1–9 (2015).

4. Fan, Y. *et al.* Extraction of phenols from water with functionalized ionic liquids. *Ind. Eng. Chem. Res.* **53**, 20024–20031 (2014).

5. Warrag, S. E., Alli, R. D. & Kroon, M. C. Liquid–liquid equilibrium measurements for the extraction of pyridine and benzothiazole from n-alkanes using deep eutectic solvents. *J. Chem. Eng. Data* **64**, 4882–4890 (2019).

6. Rogošić, M. & Kučan, K. Z. Deep eutectic solvent based on choline chloride and propylene glycol as a potential medium for extraction denitrification of hydrocarbon fuels. *Chem. Eng. Res. Des.* **161**, 45–57 (2020).

7. Nemati, M., Tuzen, M., Farazajdeh, M. A., Kaya, S. & Mogaddam, M. R. A. Development of dispersive solid-liquid extraction method based on organic polymers followed by deep eutectic solvents elution; application in extraction of some pesticides from milk samples prior to their determination by HPLC-MS/MS. *Anal. Chim. Acta* **1199**, 339570 (2022).

8. Ahmadi, R., Azooz, E. A., Yamini, Y. & Ramezani, A. M. Liquid–liquid microextraction techniques based on in-situ formation/ decomposition of deep eutectic solvents. *TrAC-Trends Anal. Chem.* **161**, 117019 (2023).

9. Farajzadeh, M. A. *et al.* Experimental and density functional theory studies during a new solid phase extraction of phenolic compounds from wastewater samples prior to GC–MS determination. *Microchem. J.* **177**, 107291 (2022).

10. Abbott, A. P. *et al.* Preparation of novel, moisture-stable, Lewis-acidic ionic liquids containing quaternary ammonium salts with functional side chainsElectronic supplementary information (ESI) available: plot of conductivity vs. temperature for the ionic liquid formed from zinc chloride and choline chloride (2: 1). *Chem. Commun.* **19**, 2010–2011 (2001).

11. van Osch, D. J., Zubeir, L. F., van den Bruinhorst, A., Rocha, M. A. & Kroon, M. C. Hydrophobic deep eutectic solvents as water-immiscible extractants. *Green Chem.* **17**, 4518–4521 (2015).

12. Kudłak, B., Owczarek, K. & Namieśnik, J. Selected issues related to the toxicity of ionic liquids and deep eutectic solvents—A review. *Environ. Sci. Pollut. Res.* **22**, 11975–11992 (2015).

13. Ghaffari, F., Khorsandi, M., Shekaari, H. & Zafarani-Moattar, M. T. Liquid–liquid equilibrium measurements and computational study of salt–polymer aqueous two phase system for extraction of analgesic drugs. *Sci. Rep.* **12**, 1–11 (2022).

14. Florindo, C., Romero, L., Rintoul, I., Branco, L. C. & Marrucho, I. M. From phase change materials to green solvents: Hydrophobic low viscous fatty acid–based deep eutectic solvents. *ACS Sustain. Chem. Eng.* **6**, 3888–3895 (2018).

15. Santos, L. B. *et al.* Deep eutectic solvents in liquid–phase microextraction: Contribution to green chemistry. *TrAC-Trends Anal. Chem.* **146**, 116478 (2022).

16. Florindo, C., Branco, L. & Marrucho, I. Development of hydrophobic deep eutectic solvents for extraction of pesticides from aqueous environments. *Fluid Phase Equilib.* **448**, 135–142 (2017).

17. Verma, R. & Banerjee, T. Liquid–liquid extraction of lower alcohols using menthol-based hydrophobic deep eutectic solvent: experiments and COSMO-SAC predictions. *Ind. Eng. Chem. Res.* **57**, 3371–3381 (2018).

18. Verma, R. & Banerjee, T. Palmitic-acid-based hydrophobic deep eutectic solvents for the extraction of lower alcohols from aqueous media: liquid-liquid equilibria measurements. *Validat. Process Econom. Glob. Chall.* **3**, 1900024 (2019).

19. Dietz, C. H., Kroon, M. C., Di Stefano, M., van Sint Annaland, M. & Gallucci, F. Selective separation of furfural and hydroxymethylfurfural from an aqueous solution using a supported hydrophobic deep eutectic solvent liquid membrane. *Faraday Discuss.* **206**, 77–92 (2018).

20. Wang, X., Lu, Y., Shi, L., Yang, D. & Yang, Y. Novel low viscous hydrophobic deep eutectic solvents liquid-liquid microextraction combined with acid base induction for the determination of phthalate esters in the packed milk samples. *Microchem. J.* **159**, 105332 (2020).

21. Sas, O. G., Castro, M., Domínguez, Á. & González, B. Removing phenolic pollutants using deep eutectic solvents. *Sep. Purif. Technol.* **227**, 115703 (2019).

22. Cea-Klapp, E. *et al.* Separation of furfuryl alcohol from water using hydrophobic deep eutectic solvents. *J. Mol. Liq.* **384**, 122232 (2023).

23. Pochivalov, A. *et al.* Liquid–liquid microextraction with hydrophobic deep eutectic solvent followed by magnetic phase separation for preconcentration of antibiotics. *Talanta* **252**, 123868 (2023).

24. Arcon, D. P. & Franco, F. C. Jr. All-fatty acid hydrophobic deep eutectic solvents towards a simple and efficient microextraction method of toxic industrial dyes. *J. Mol. Liq.* **318**, 114220 (2020).

25. Shekaari, H. & Mousavi, S. S. Volumetric properties of ionic liquid 1, 3-dimethylimidazolium methyl sulfate+ molecular solvents at T=(298.15–328.15) K. *Fluid Phase Equilib.* **291**, 201–207 (2010).

26. Domingues, L., Cussolin, P. A., da Silva, J. L., de Oliveira, L. H. & Aznar, M. Liquid–liquid equilibrium data for ternary systems of water+ lactic acid+ C4–C7 alcohols at 298.2 K and atmospheric pressure. *Fluid Phase Equilib.* **354**, 12–18 (2013).

27. Saien, J. & Razi Asrami, M. Liquid–liquid equilibrium of the ternary system of water+ phenol+(propan-2-yl) benzene at several temperatures. *J. Chem. Eng. Data* **62**, 3663–3670 (2017).

28. Lide, D. R. *CRC Handbook of Chemistry and Physics* (CRC Press, Boca Raton, Florida, 2004).

29. Saien, J., Daliri, S. & Norouzi, M. Liquid–liquid equilibria for the system water + 4-methylpentan-2-one + acetic acid at several temperatures. *J. Chem. Eng. Data* **57**, 2553–2559 (2012).

30. Chen, Y. *et al.* Liquid– liquid equilibria of aqueous biphasic systems composed of 1-butyl-3-methyl imidazolium tetrafluoroborate + sucrose/maltose + water. *J. Chem. Eng. Data* **55**, 3612–3616 (2010).

31. Arce, A., Arce, A. Jr. & Rodriguez, O. Revising concepts on liquid–liquid extraction: data treatment and data reliability. *J. Chem. Eng. Data* **67**, 286–296 (2021).

32. Pir, M., Ghanadzadeh Gilani, A. & Mohammadi-Khanghah, B. Liquid–liquid equilibria in aqueous mixtures of phosphoric acid with two primary aryl alcohols at T=(298.2, 308.2, and 318.2) K: measurements and correlation. *J. Solut. Chem.* **50**, 73–89 (2021).

33. Mascietti, V. A., Farias, L. S., Tavares, F. W. & Ndiaye, P. M. Liquid–liquid equilibria of ternary mixtures of methanol + MEG + n-C₅, ethanol + MEG + n-C₅, and n-butanol + MEG + n-C₅. *Can. J. Chem. Eng.* **101**, 3512–3521 (2023).

34. Hadj-Kali, M. K., Salleh, Z., Ali, E., Khan, R. & Hashim, M. A. Separation of aromatic and aliphatic hydrocarbons using deep eutectic solvents: A critical review. *Fluid Phase Equilib.* **448**, 152–167 (2017).

35. Magnussen, T., Sørensen, J. M., Rasmussen, P. & Fredenslund, A. Liquid-liquid equilibrium data: Their retrieval, correlation and prediction Part III: Prediction. *Fluid Phase Equilib.* **4**, 151–163 (1980).

36. Saien, J., Asrami, M. R. & Salehzadeh, S. Phase equilibrium measurements and thermodynamic modelling of water+ phenol+[Hmim][NTf2] ionic liquid system at several temperatures. *J. Chem. Thermodyn.* **119**, 76–83 (2018).

37. Huang, F. *et al.* Surfactant-based ionic liquids for extraction of phenolic compounds combined with rapid quantification using capillary electrophoresis. *Electrophor.* **35**, 2463–2469 (2014).

38. Pan, L. *et al.* Extraction of bisphenol F three isomers from water with 1-octyl-3-methylimidazolium tetrafluoroborate ionic liquid. *Can. J. Chem. Eng.* **95**, 516–523 (2017).

39. Saien, J., Badieh, M. M. S., Norouzi, M. & Salehzadeh, S. Ionic liquid 1-hexyl-3-methylimidazolium hexafluorophosphate, an efficient solvent for extraction of acetone from aqueous solutions. *J. Chem. Thermodyn.* **91**, 404–413 (2015).

40. Liu, D., Luo, L., Li, L. & Chen, Y. Liquid–liquid equilibria for the methyl tert-butyl ketone+ phenol+ water ternary system at 298.15, 313.15 and 323.15 K. *J. Solut. Chem.* **44**, 1891–1899 (2015).

41. Yuan, X. & Chen, Y. Experimental study of liquid–liquid equilibria for systems of (dibutyl ether+ phenol+ water) at different temperatures. *J. Chem. Thermodyn.* **152**, 106261 (2021).

42. Gilani, H. G., Gilani, A. G. & Sangashekan, M. Tie-line data for the aqueous solutions of phenol with organic solvents at T= 298.2 K. *J. Chem. Thermodyn.* **58**, 142–148 (2013).
43. Liu, D., Li, L., Lv, R. & Chen, Y. Liquid–liquid equilibria for the ternary system mesityl oxide+ phenol+ water at 298.15, 313.15, and 323.15 K. *J. Chem. Eng. Data* **61**, 2493–2498 (2016).
44. Cesari, L., Canabady Rochelle, L. & Mutelet, F. Extraction of phenolic compounds from aqueous solution using choline bis (trifluoromethylsulfonyl) imide. *Fluid Phase Equilibr.* **446**, 28–35 (2017).
45. Mirza, N. R., Nicholas, N. J., Wu, Y., Kentish, S. & Stevens, G. W. Estimation of normal boiling temperatures, critical properties, and acentric factors of deep eutectic solvents. *J. Chem. Eng. Data* **60**, 1844–1854 (2015).
46. Alvarez, V. & Valderrama, J. A modified Lydersen-Joback-Reid method to estimate the critical properties of biomolecules. *Alimentaria* **254**, 55–66 (2004).
47. Simoni, L. D., Lin, Y., Brennecke, J. F. & Stadtherr, M. A. Modeling liquid–liquid equilibrium of ionic liquid systems with NRTL, electrolyte-NRTL, and UNIQUAC. *Ind. Eng. Chem. Res.* **47**, 256–272 (2008).
48. Chen, B., Wu, Y., Suo, M. & Yang, S. Liquid–liquid equilibrium and data correlation for quaternary (methyl isobutyl ketone + n-pentanol + phenol + water) system at 101 kPa and 298.2 K: phenol coextraction with synergistic solvents. *J. Chem. Eng. Data* **65**, 4567–4574 (2020).
49. Banerjee, T., Singh, M. K., Sahoo, R. K. & Khanna, A. Volume, surface and UNIQUAC interaction parameters for imidazolium based ionic liquids via Polarizable Continuum Model. *Fluid Phase Equilib.* **234**, 64–76 (2005).

Acknowledgements

Author contributions

J.S.: Methodology, supervision, review and editing. M.B.: Experiments, conceptualization, methodology, investigation. F.J.: Experiments, editing, software, evaluating.

Competing interests

The authors declare no competing interests.

Additional information

Supplementary Information The online version contains supplementary material available at https://doi.org/10.1038/s41598-023-44600-x.

Correspondence and requests for materials should be addressed to J.S.

Reprints and permissions information is available at www.nature.com/reprints.

Publisher's note Springer Nature remains neutral with regard to jurisdictional claims in published maps and institutional affiliations.